G. Physical processes and diffusion

G-1. Cloud microphysics

G-1-1 General features of cloud microphysics

The explicit cloud scheme of the model is basically the same as that in Ikawa *et al.* (1991) and Ikawa and Saito (1991), where the water substances are categorized into six species (water vapor, cloud water, rain, cloud ice, snow and graupel). The cloud microphysical processes are illustrated in Fig. G1-1-1. This scheme is based on the formulation of Lin *et al.* (1983) but has an option that predicts not only the mixing ratios of the six water species but also the number concentrations of three ice species (cloud ice, snow and graupel), referring to Murakami (1990). For the details, see B-11 of Ikawa and Saito (1991).

G-1-2 Box-Lagrangian raindrop scheme

When a prognostic explicit scheme is employed in numerical models with a horizontal grid size larger than 10 km, the rain terminal velocity V, not the air horizontal velocity, restricts the time step interval Δt. In those models, Δt must be chosen independent of horizontal grid spacing Δx to satisfy the Courant-Friedrich-Lewy (CFL) condition for rain falling ($V\Delta t/\Delta z<1$, where Δz is the vertical grid interval). Especially when many vertical layers are employed in the lower part of the domain to express the atmospheric boundary layer in detail, Δt has to be so reduced to calculate stable rain fall. Actually, for 10 to 20 km grid-resolution models in which

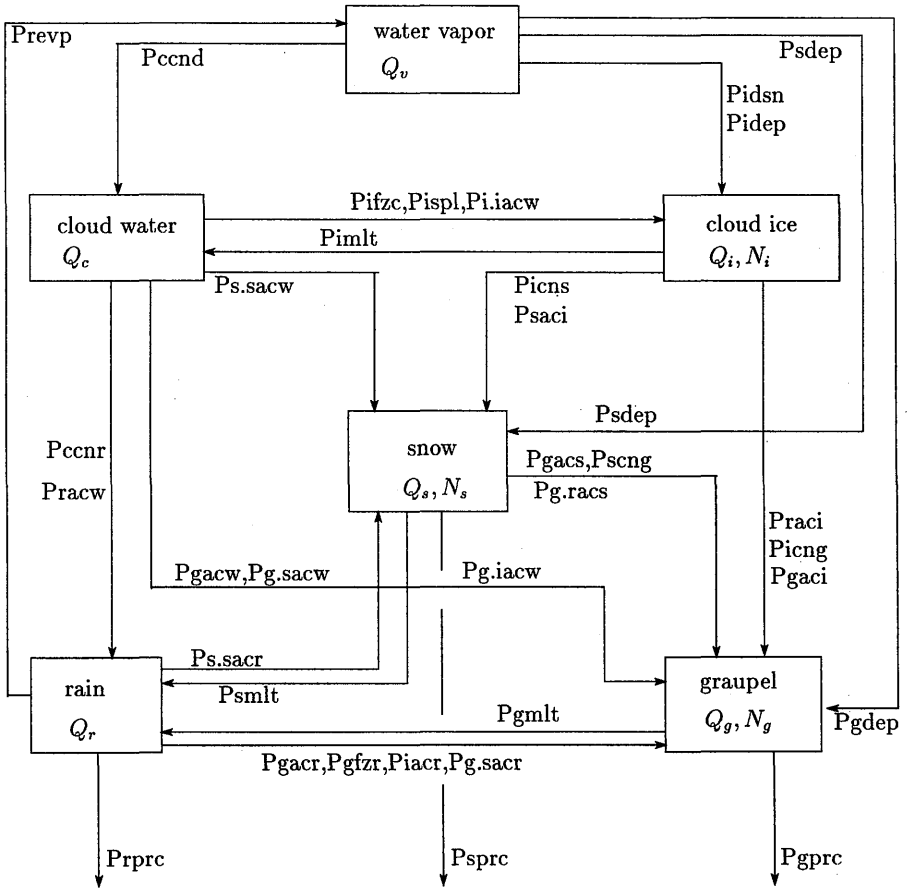

Fig. G1-1-1 Cloud microphysical processes in the model. Reproduced from Ikawa and Saito (1991). For explanation of the symbols, see B-11-1 in Ikawa and Saito (1991).

a prognostic explicit scheme is employed, $\Delta t=15$ to 30 sec has been used (*e.g.,* Yamasaki, 1977 ; Kato and Saito, 1995).

In numerical models with a grid size larger than 10 km, to use the time step interval calculated from the CFL condition for air advection (*i.e.,* $Va\ \Delta t/\Delta x<1$, where Va is the absolute value of air horizontal velocity), a new raindrop scheme named the Box-Lagradian raindrop scheme was developed (Kato, 1996). This new scheme is described in this section. First, a raindrop scheme is designed from the following equation when it is assumed anelastic.

$$\rho\frac{dq}{dt}=\rho\frac{\partial q}{\partial t}-\frac{\partial(\rho qV)}{\partial z}=0. \qquad \text{(G1-2-1)}$$

Here, ρ is the air density, q is the mixing ratio of rainwater and V is the rain terminal velocity defined as $V=Aq^n$, where A and n are positive constants. In numerical models, the amount at the next time step is generally calculated from $\rho\frac{\partial q}{\partial t}=\frac{\partial(\rho qV)}{\partial z}$ (the Eulerian method), but a method that searches for dropping points after a time step interval by using the left-hand side of (G1-2-1) (the Lagrangian method) is considered. The new raindrop scheme is based on the Lagrangian method, but it drops the bulk of rainwater in a vertical gird box, not the rainwater at a vertical grid point. Figure G1-2-1 outlines the new scheme. It is designed so that the bulk of rainwater $\rho q\Delta z$ in a vertical grid box, which is defined by two vertical layers, is preserved while keeping V

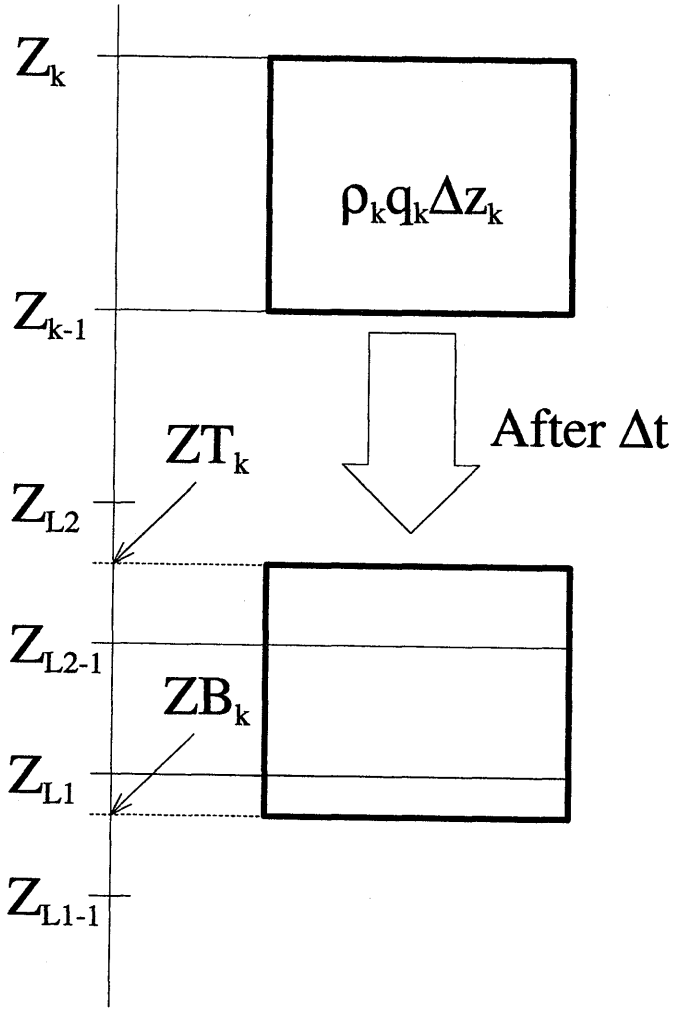

Fig. G1-2-1 Outline of box-Lagrangian raindrop scheme (from Kato, 1996).

constant during a time step interval Δt. The k-th vertical grid box is displaced downward during a time step interval, and the heights of the top ZT_k, and the bottom ZB_k of the k-th grid box after displaced are determined first.

The vertical layer where ZT_k or ZB_k exists is then searched:

$$\begin{aligned} &ZT_k^m = Z_k - V_k^m \Delta t \quad \in [Z_{L2-1}, Z_{L2}], \\ \text{and} \quad &ZB_k^m = Z_{k-1} - V_k^m \Delta t \quad \in [Z_{L1-1}, Z_{L1}], \end{aligned} \tag{G1-2-2}$$

where Z_k is the top height of the k-th vertical grid box, the superscript 'm' denotes the value at the time step 'm' and the brackets $[T,B]$ represent the interval in space between T and B.

Next, the dropped bulk of rainwater is partitioned into vertical grid boxes between ZT_k and ZB_k. When the displaced box interacts with the ground surface, the rainwater below it is removed from the model domain as precipitation. For $L1 \neq L2$,

$$\begin{aligned} &P_{L1,k}^{m+1} = \rho_k q_k^m (Z_{L1} - ZB_k), \\ &P_{L,k}^{m+1} = \rho_k q_k^m (Z_L - Z_{L-1}) \qquad \text{for } L1 < L < L2, \end{aligned}$$

and (G1-2-3)

$$P_{L2,k}^{m+1} = \rho_k q_k^m (ZT_k - Z_{L2-1}),$$

for $L1 = L2$,

$$P_{L1,k}^{m+1} = \rho_k q_k^m \Delta z_k, \tag{G1-2-4}$$

where $P_{L,k}^{m+1}$ is the dropped rainwater in the L-th grid box at the next time step from the k-th grid box, and the subscript 'k' denotes the value at the k-the vertical grid point. Summing the dropped rainwater from all vertical grid boxes, the mixing ratio of rainwater at the next time step is calculated as

$$q_L^{m+1} = \frac{\sum_k P_{L,k}^{m+1}}{\rho_L (Z_L - Z_{L-1})}. \tag{G1-2-5}$$

When the CFL condition ($\Delta z > V \Delta t$) is satisfied, $L1 = k\text{-}1$ and $L2 = k$ are obtained from (G1-2-2). By substituting $L1 = k\text{-}1$ and $L2 = k$ into (G1-2-3) and (G1-2-5), the change of q per unit time, $\left(\frac{\partial q}{\partial t}\right)_k^m$, is obtained as

$$\left(\frac{\partial q}{\partial t}\right)_k^m = \frac{\frac{P_{k,k+1}^{m+1} + P_{k,k}^{m+1}}{\rho_k (Z_k - Z_{k-1})} - q_k^m}{\Delta t} = \frac{\rho_{k+1} q_{k+1}^m V_{k+1}^m - \rho_k q_k^m V_k^m}{\rho_k (Z_k - Z_{k-1})}. \tag{G1-2-6}$$

In contrast, from (G1-2-1), $\left(\frac{\partial q}{\partial t}\right)_k^m$ in the Eulerian raindrop scheme is given as

$$\left(\frac{\partial q}{\partial t}\right)_k^m = \frac{\partial (\rho q V)_k^m}{\rho_k \partial z_k} = \frac{(\rho q V)_{k+1}^m - (\rho q V)_k^m}{\rho_k \Delta z_k}. \tag{G1-2-7}$$

Thus, from (G1-2-6) and (G1-2-7), the box-Lagrangian and the Eulerian schemes coincide with each other when the CFL condition is satisfied.

G-1-3 Moist convective adjustment

The moist convective adjustment was originally proposed by Manabe *et al.* (1965). A scheme modified by Gadd and Keers (1970) is adopted in the MRI-NHM. The modified scheme has the following processes. If the temperature lapse rate exceeds the critical value Γ_c and the relative humidity RH exceeds its intermediate value

RH_i (0.5 is used in the model), temperature and specific humidity are adjusted so that the lapse rate becomes Γ_c while conserving relative humidity and total thermal energy. Γ_c is a function of relative humidity defined as

$$\Gamma_c=\frac{1}{1-RH_i}(\Gamma_d(1-RH)+\Gamma_s(RH-RH_i)) \quad for \quad RH_i<RH, \tag{G1-3-1}$$

where Γ_d and Γ_s are the dry adiabatic lapse rate and the saturated lapse rate. If only a moist convective adjustment scheme is employed in the model as a rain-generation process, the supersaturation Δs produced by the adjustment of specific humidity is forced to drop to the ground during the time step interval. In the MRI-NHM, however, Δs can be held on the grid scale since the moist convective adjustment scheme can be used in conjunction with the prognostic explicit scheme. Therefore, the following two cases are examined.

Case 1. The supersaturation Δs yielded by the moist convective adjustment is instantaneously removed from the model grids as precipitation.

Case 2. Δs is shared equally to the mixing ratio of cloud water q_c in adjusted grids as follows:

$$q_{c,k}\rightarrow q_{c,k}+\frac{\Delta s}{\sum_{n=k1}^{k2}\rho_n\Delta Z_n}, \quad \Delta s=\sum_{n=k1}^{k2}\rho_n\Delta q_n\Delta Z_n, \quad for \quad k1\leq k\leq k2, \tag{G1-3-2}$$

where Δq_k is the adjusted amount at the k-th vertical layer and $k1$ and $k2$ indicate the bottom and top of adjusted layers, respectively.

When a moist convective adjustment scheme is used in conjunction with an explicit precipitation scheme, the temperature change ΔT adjusted by the former scheme must be modified dependently on the model grid-resolution Δx and the convective time scale so that the conjunction scheme is reduced to an explicit scheme for small Δx and Δt:

$$\Delta T\rightarrow\frac{\Delta x-1km}{19km}\times\frac{\Delta t}{20\ \mathrm{min}}\times\Delta T \quad for \quad 1km<\Delta x<20km,$$

and

$$\Delta T\rightarrow\frac{\Delta t}{20\ \mathrm{min}}\times\Delta T \quad for \quad \Delta x\geq 20km, \tag{G1-3-3}$$

where Δt is the time step interval.

G-1-4 Cloud amount prediction scheme

Cloud water advected by saturated air flow never evaporates if the temperature of the air is not increased. In the computational domain where a grid method is used, cloud water that moves into a grid box where the air is not saturated is instantly evaporated. This often occurs in grid boxes neighboring a cloud. In order to suppress this erroneous evaporation, cloud amounts are employed as follows.

For convenience, the one-dimensional case is described here. The cloud amount C_m is advected by using a modified upstream scheme as

$$C_{m,j}^{m+1}=Min\left(1.0,\ C_{m,j}^{m-1}-2\Delta t\frac{N_{i+\frac{1}{2}}^{m}u_{i+\frac{1}{2}}^{m}-N_{i-\frac{1}{2}}^{m}u_{i-\frac{1}{2}}^{m}}{\Delta x}\right), \tag{G1-4-1}$$

where the superscript "m" denotes the m-th time step, Δx is the grid interval, and Δt is the time step interval.

The value of N is determined by the following conditions as

$$N^{m}_{i-\frac{1}{2}}=0 \quad for \quad C^{m-1}_{m,j-1}\neq 1, \quad C^{m-1}_{m,j}=0, \quad u^{m}_{i-\frac{1}{2}}>0,$$

$$N^{m}_{i+\frac{1}{2}}=0 \quad for \quad C^{m-1}_{m,j+1}\neq 1, \quad C^{m-1}_{m,j}=0, \quad u^{m}_{i-\frac{1}{2}}<0,$$

and (G1-4-2)

$$N^{m}_{i\pm\frac{1}{2}}=1 \quad for\ other\ cases.$$

When the air in a grid box is determined as saturated after calculating condensation and evaporation between water vapor q_v and cloud water q_c using an "instantaneous adjustment procedure," C_m is set to 1.0 independently of the advection result. When C_m becomes negative after calculation by (G1-4-1), C_m and q_c are adjusted as follows. C_m is set to 0.0, and q_c is moved into the neighboring grid box on the windward side when the air in the box is saturated; otherwise, C_m is set to 1.0 in order to accelerate the evaporation of cloud water. For two- or three-dimension simulation, when there are several neighboring grid boxes into which q_c can be moved, q_c is equally divided among these grid boxes.

The evaporation of cloud water during the "instantaneous adjustment procedure" is restricted by C_m. The values of cloud water q_c^* and cloud amount C_m^* after this evaporation are calculated as

$$q^*_c = Max\left(q_c-(q_{vs}-q_v)\,C_m,\ q_c(1.0-C_m)\right), \tag{G1-4-3}$$

$$C^*_m = C_m\frac{q^*_c}{q_c}, \tag{G1-4-4}$$

where q_{vs} is the saturated mixing ratio of water vapor. For $C_m=1.0$, (G1-4-3) gives the original values. The first term on the right-hand side of (G1-4-3) means that the evaporation of cloud water is restricted to only the region where cloud water exists in a grid box. The second term determines the maximum evaporation of cloud water. Furthermore, cloud water is restricted to evaporate only in downdrafts. Under these restrictions, the finite difference form for the advection of cloud water is modified as

$$q^{m+1}_{c,i}=q^{m-1}_{c,i}-2\Delta t\frac{N^{m}_{i+\frac{1}{2}}u^{m}_{i+\frac{1}{2}}q^{m}_{c,j+\frac{1}{2}}-N^{m}_{i-\frac{1}{2}}u^{m}_{i-\frac{1}{2}}q^{m}_{c,j-\frac{1}{2}}}{\Delta x}. \tag{G1-4-5}$$

G-2. Surface Boundary layer

G-2-1 Surface fluxes

A surface boundary layer is assumed at the lower boundary, where the resistance law gives surface heat and momentum fluxes. Over the sea, exchange coefficients are determined from the formula by Kondo (1975); over land, they are based on Monin and Obukhov's similarity law with Sommeria's (1976) formula, depending on the ground roughness and ground (sea-surface) temperature. The above formulations are the same as in B-10-2 of Ikawa and Saito (1991), while the ground temperatures of four soil layers are predicted as described in next subsection.

P.G. The surface fluxes are computed in sub.CRSTUV. The drag coefficients are calculated in sub.KONDOH and sub.GRDFXH on the sea and land, respectively.

G-2-2 Ground temperature

According to Segami *et al.* (1989), we use the four-layer model shown in Fig. G.2.1 to predict ground temperature. The predictive equation of underground temperature T is given as

$$\rho_c \frac{\partial T}{\partial t} = -\frac{\partial G}{\partial z}, \tag{G2-2-1}$$

$$G = -\lambda \frac{\partial T}{\partial z}, \tag{G2-2-2}$$

where λ is the thermal conductivity and ρ_c, the heat capacity. Finite discretization forms of (G2-2-1) and (G2-2-2) are expressed as follows.

$$G_k = 2\lambda \frac{T_{k-1} - T_k}{\Delta z_{k-1} + \Delta z_k}, \tag{G2-2-3}$$

$$\frac{\partial T_k}{\partial t} = -\frac{G_k - G_{k-1}}{\rho_c \Delta z_k}, \tag{G2-2-4}$$

where Δz_k is the depth of the k-th layer. T_4 is assumed constant during the forecast. The heat balance at the ground surface G_1 is given as

$$G_1 = -\varepsilon\sigma T_1^4 - H - LE + (1-\alpha) R_s + R_L, \tag{G2-2-5}$$

where ε (=0.95) is the emissivity of the ground surface, σ the Stefan-Boltzman constant, H the latent heat, LE the sensitive heat, α the albedo of the ground surface, R_s the solar radiation reaching the ground, and R_L the downward long wave radiation at the ground surface. H and LE are calculated from Eqs. 8-7 and 8-8 in Ikawa and Saito (1991), respectively. R_s and R_L are obtained by using an atmospheric radiation scheme described in section G-5. When the atmospheric radiation is not calculated in the model, R_s and R_L are expressed as the following formula proposed by Kondo (1976):

$$R_s = S(1-0.7C_L)(1-0.6C_M)(1-0.3C_H), \tag{G2-2-6}$$

$$S = S_\infty \cos\zeta \{0.57 - 0.016e - 0.06\log_{10} e + (0.43 + 0.016e) \times 10^{-0.13\sec\zeta}\}, \tag{G2-2-7}$$

$$\cos\zeta = \sin\theta \sin\theta_s + \cos\theta \cos\theta_s \cos\phi_t, \tag{G2-2-8}$$

$$R_L = \varepsilon\sigma T_a^4 [1 + (-0.49 + 0.066e)\{1 - (0.75 - 0.0005e)(C_L + 0.85C_M + 0.5C_H)\}], \tag{G2-2-9}$$

where S_∞ is the solar constant, θ the latitude, θ_s the declination, ϕ_t the hour angle, e the water vapor pressure near the ground surface, and T_a the temperature near the ground surface. C_L, C_M and C_H indicate the amount of low, middle and high clouds. They are calculated with the relative humidity averaged between the ground surface and 1.5 km height (low cloud), 1.5 and 5.0 km height (middle cloud), and 5.0 and 10.0 km height (high cloud) by using the empirical formula proposed by Ohno and Isa (1984).

The surface temperature at the time step "$m+1$" T_1^{m+1} can be calculated from (G2-2-3) and (G2-2-4), after G_1^m and G_1^{m+1} are obtained from (G2-2-5) for a given T_4. Here G_1^{m+1} is calculated by using the trapezoid implicit method shown below.

$$G_1^{m+1} = G_1^m + \left(\Delta t \frac{\partial G_1}{\partial t}\right)^{m+\frac{1}{2}} = G_1^m + \left(\Delta t \frac{\partial G_1}{\partial T_1}\frac{\partial T_1}{\partial t}\right)^{m+\frac{1}{2}} \approx G_1^m + \left(\frac{\partial G_1}{\partial T_1}\right)^m (T_1^{m+1} - T_1^m). \tag{G2-2-10}$$

The orographic steepness increases or decreases the solar radiation reaching the ground. To introduce this effect into the model, the zenith angle ζ is modified in a north-south direction based on the alteration of latitude (Fig. G2-2-2a) as

$$\theta \rightarrow \theta + \tan^{-1}\frac{\partial z}{\partial y} \qquad \text{(G2-2-11)}$$

and in an east-west direction based on the alteration of hour angle (Fig. G2-2-2b) as

$$\phi_t \rightarrow \phi_t + \tan^{-1}\frac{\partial z}{\partial x}, \qquad \text{(G2-2-12)}$$

Here, ζ is not modified for $\cos\zeta < 0$ (*i.e.*, the grids on which the Earth throws a shadow).

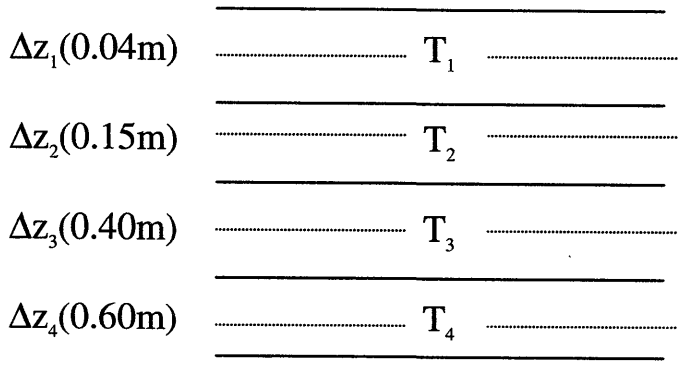

Fig. G2-2-1 Layers underground. T_k and Δz_k are the underground temperature and the depth of the k-th layer.

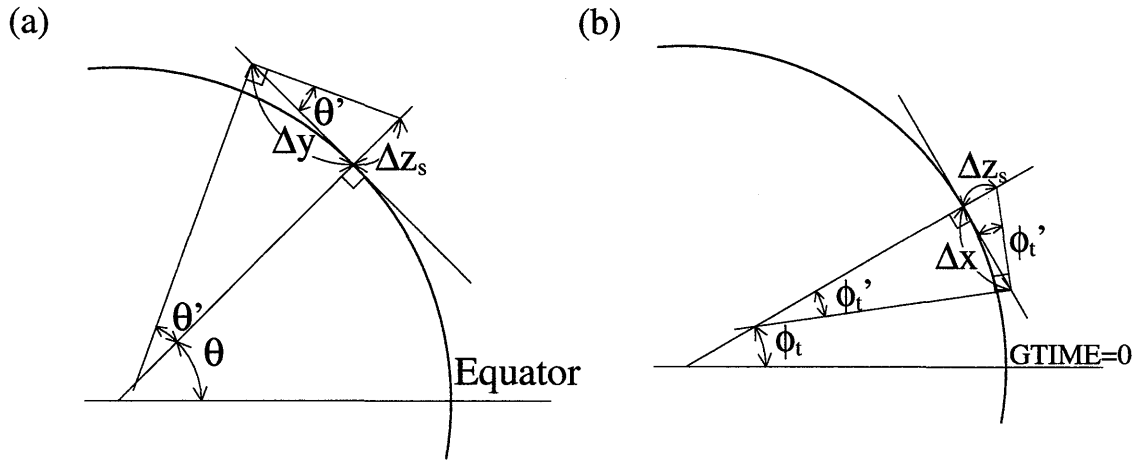

Fig. G2-2-2 Alteration of (a) latitude and (b) hour angle for the modification of the zenith angle.

G-3. Turbulent closure model

The turbulent closure model that predicts the turbulent kinetic energy is employed to determine the diffusion coefficients. The formulation is based on Klemp and Wilhelmson (1978) and Deardorff (1980), but slightly modified. For details, see B-10-1 of Ikawa and Saito (1991). In the model, the linear stability condition

$$K < K_{\max}(z) = 0.1\left(\cong\frac{1}{\pi^2}\right)\frac{(\Delta z)^2}{\Delta t}, \qquad \text{(G3-1)}$$

is imposed for the eddy diffusion coefficients K_m, K_e and K_h in order to maintain a stable run.

P.G. The surface fluxes are computed in sub.CRSTUV. The turbulent energy is computed in sub.CETUR5. K_{max} is set in sub.SETEMX.

G-4. Computational diffusion

A nonlinear damper, a fourth-order linear damper, and Asselin's time filter are employed to suppress the computational noise, adding to the Rayleigh damping (F2-4-1) and (F3-2-1).

a. Non- linear damper

Nonlinear damping (Nakamura, 1978)

$$D_{NL}=\frac{1}{m_{NL}\Delta t}\{(\Delta x)^3\frac{\partial}{\partial x}(\left|\frac{\partial\phi}{\partial x}\right|\frac{\partial\phi}{\partial x})+(\Delta y)^3\frac{\partial}{\partial y}(\left|\frac{\partial\phi}{\partial y}\right|\frac{\partial\phi}{\partial y})\}, \tag{G4-1}$$

is added to the diffusion term of ϕ, where m_{NL} is the coefficient that determines the $1/e$-folding time. For two-grid noises of amplitude a, (G4-1) gives the equivalent $1/e$-folding time $m_{NL}\Delta t/8a$. In above expression, the uniform horizontal grid distances are assumed.

b. Fourth-order linear damper

Fourth-order linear damping

$$D_{2D}=-\frac{1}{m_{2D}\Delta t}\{(\Delta x)^4\frac{\partial^4\phi}{\partial x^4}+(\Delta y)^4\frac{\partial^4\phi}{\partial y^4}\}, \tag{G4-2}$$

where m_{2D} is the coefficient which determines the e-folding time, is added to the diffusion term of ϕ to suppress primarily two-grid noises. For two-grid noises whose amplitude is a, (G4-2) gives the equivalent $1/e$-folding time $m_{2D}\Delta t/16$. In the above expression, the uniform grid distances are assumed horizontally. Currently, this diffusion is not employed at the lateral boundaries and their inner next grid points in order to assure symmetry.

c. Asselin's time filter

After the time integration, all quantities of prognostic variables at the time step '*it*' are modified according to the Asselin's time filter (Robert, 1966),

$$\phi(,,,it)\rightarrow\phi(,,,it)+0.5\nu(\phi(,,,it+1)-2\phi(,,,it)+\phi(,,,it)+\phi(,,,it-1)\}, \tag{G4-3}$$

where ν is the coefficient set by the input parameter card (usually 0.2). Near the upper boundary ($kz>0.7*NZ$), ν is increased linearly up to three times of the original value.

P.G. Linear and nonlinear dampers are computed in sub.DAMPCN. The time filter is employed in sub. TSMOTH, using the quantities at the time step "*it*-1" that is set by sub.OSAVEH.

G-5. Atmospheric Radiation

G-5-1 Atmospheric radiation calculated using relative humidity.

The basic framework of the radiation scheme was described by Sugi *et al.* (1990), and the introduced scheme in MRI-NHM was developed with reference to the software package in JSM. Full computation of long wave radiation is made with an interval that can be determined by a control parameter card (see subsection K-4-3). The following description is referred to subsection 3.2.3 in NPD/JMA (1997). Only long-wave flux radiated from the ground surface is considered in every time step. The temperature tendency relates to radiative fluxes

$$\left(\frac{\partial T}{\partial t}\right)_{rad}=-\frac{RT}{C_p p}\frac{\partial F}{\partial z}, \tag{G5-1-1}$$

where F is the net upward flux.

(a) Long-wave flux

The long-wave flux F can be written as

$$F=C(z,z_s)\,\tau(s,T_s)\{\pi B(T_g)-\pi B(T_s)\}+C(z,z_t)\,\tau(s_t-s,\,T_t)\,\pi B(T_t)$$

$$+\int_{T_t}^{T_g} C(z,z')\,\tau^*(|s-s'|,\,T')\frac{d\pi B(T')}{dT'}dT', \qquad \text{(G5-1-2)}$$

where $C(z,\,z')$ is the ratio of the clear line of sight between levels of z and z', T_g the soil temperature at the ground surface, T_s the air temperature at the ground surface, and T_t the air temperature at the top. This ratio is unity when there are no clouds. The scheme assumes that clouds are fully opaque and overlap randomly in the vertical direction. The transmission function τ and $B(T)$ are given by

$$\tau(s,T)=\frac{1}{B(T)}\int_0^\infty \tau_v(s)\,B_v(T)\,dv \qquad \text{(G5-1-3)}$$

$$\tau^*(s,T)=\frac{1}{\dfrac{dB(T)}{dT}}\int_0^\infty \tau_v(s)\frac{\partial B_v(T)}{\partial T}dv \qquad \text{(G5-1-4)}$$

and

$$\pi B(T)=\pi\int_0^\infty B_v(T)\,dv=\sigma T^4. \qquad \text{(G5-1-5)}$$

where $B_v(T)$ is the Planck function. In the model, $\tau(s,\,T)$ and $\tau^*(s,\,T)$ are selected from tables prepared in advance. To make the tables, τ_v is evaluated for each absorber assuming Goody's random model (1952). Parameters used in the random model are found in Roger and Walshaw (1966) for water vapor, Goldman and Kyle (1968) for ozone, and Houghton (1977) for carbon dioxide. The pressure broadening of each absorber (i) is considered using the scaling

$$s_i=1.66\int_0^z\left(\frac{p}{1000hPa}\right)^n\rho_i dz, \qquad \text{(G5-1-6)}$$

where the constant n is 1.0 for water vapor, 0.9 for carbon dioxide, and 0.4 for ozone. The diffusive factor of 1.66 comes from the average over all directions. is The continuum band by dimer $(H_2O)_2$ is an exception to (G5-1-6). Since the dimer is composed of two molecules, the optical density is quadratic to water vapor density (Roberts *et al.*, 1976). The transmission function is calculated in each band shown in Fig. G5-1-1 and combined

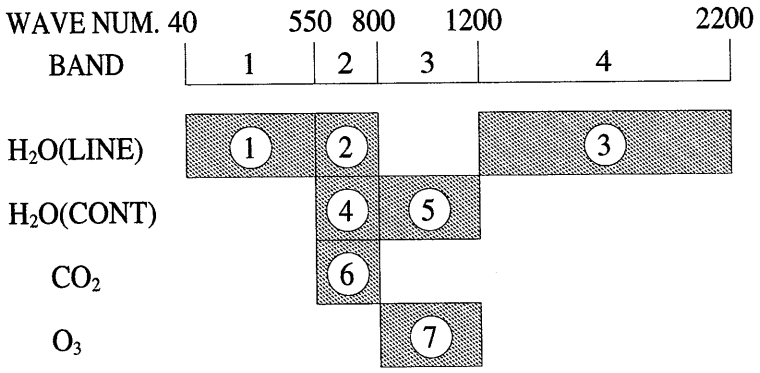

Fig. G5-1-1 Division of the wave number region for computing the transmission function. H_2O(LINE) denotes absorption due to water vapor absorption lines. H_2O(CONT) denotes the continuum band of water vapor (dimer).

to yield the total transmissivity including overlapping effects of different absorbers. In the present scheme, the absorption of dimers with wave numbers between 800 and 1200 is neglected. However, since this absorption is not small, the scheme should be modified in the near future.

(b) Short waves

The radiative processes of solar short waves are separately parameterized for wavelengths less than 0.9 μm (almost visible) and wavelengths greater than 0.9 μm (near infrared).

As to visible radiation, the scheme considers the absorption by ozone, Rayleigh scattering by air, and Mie scattering by cloud droplets. The absorber ozone exists mainly in the stratosphere. In the troposphere, complicated scattering takes place, but the heating rate due to visible radiation is quite small. Thus, the important matter for the visible radiation scheme is to evaluate precisely the reflectivity of the whole troposphere, which affects the upward stratospheric flux.

Absorbers of the near infrared band considered in the model are water vapor and cloud droplets. Lacis and Hansen (1974) expanded the transmission due to water vapor for a sum of the several bands with respect to absorption coefficients

$$\tau=\sum a_i \exp(-\lambda_i S). \qquad \text{(G5-1-7)}$$

The cloud droplets contribute both to absorption and scattering. The single scattering albedo ω_0 is assumed to be constant.

$$\omega_0=\frac{\delta_c}{(\delta_{wv}+\delta_c+\delta_l)}, \qquad \text{(G5-1-8)}$$

where the spectral dependence is neglected. Here, δ is the optical thickness, wv the absorption by water vapor, c the scattering by clouds, and l the absorption by clouds. The total thickness for near infrared radiation is

$$\delta=\delta_{wv}+\delta_c+\delta_l. \qquad \text{(G5-1-9)}$$

Both absorption and scattering are significant in the tropospheric radiative processes in the near-infrared band. These processes are calculated with the two-stream method (δ-Eddington approximation), assuming a horizontally uniform distribution of cloud droplets within each grid.

(c) Cloud fraction

The cloud fraction is one of the key factors of long- and short-wave radiative processes. The model parameterizes the cloud fraction using a quadratic function of relative humidity

$$Cloud\ fraction \propto \begin{cases} (RH-RHCC)^2 & RH > RHCC \\ 0 & RH \leq RHCC \end{cases}, \qquad \text{(G5-1-10)}$$

where the critical relative humidity $RHCC$ is empirically determined through comparison with satellite observations for the Far East region (Saito and Baba, 1988). The $RHCC$ should be re-determined for other regions. The proportional constant of (G5-1-10) is tuned for the model to reproduce realistic outgoing long-wave radiation and planetary albedo.

G-5-2 Atmospheric radiation for cloud resolving model

This radiation scheme was originally proposed by Yamamoto and Satomura (1994). The basic framework

of this scheme is almost the same as that of subsection G-5-1. MRI-NHM calculates cloud properties directly, so parameterization of the radiative properties of clouds can be introduced. In this scheme, the liquid water path (LWP) and ice water path (IWP) are used as the basic parameters for computing the radiative properties of clouds.

(a) Shortwave parameterization

In this parameterization of the solar radiative properties of clouds, optical thickness τ is expressed in terms of LWP or IWP. Formulations by Stephens (1978) are used for water clouds. In this scheme, τ and LWP are related as follows:

(i) Wavelength $<0.9\ \mu$m (almost visible)

$$\log_{10}\tau = 0.2633 + 1.7095\ln(\log_{10} LWP). \qquad \text{(G5-2-1)}$$

(ii) Wavelength $>0.9\ \mu$m (near infrared).

$$\log_{10}\tau = 0.3492 + 1.6518\ln(\log_{10} LWP). \qquad \text{(G5-2-2)}$$

From Liou (1992), the parameterization of optical thickness involving ice clouds is written in the form

$$\tau = IWP(-6.6560\times10^{-3} + 3.6860\times10^{0}/D_e), \qquad \text{(G5-2-3)}$$

where D_e is the mean effective radius; that value is fixed to 100 μm in this model.

(b) Longwave parameterization

In this scheme, cloud emittance is calculated from LWP or IWP, and it substitutes for cloud coverage in the scheme of subsection G-5-1. Neglecting the scattering contribution and applying the gray approximation, the broadband emittance ε of clouds may be expressed by

$$\varepsilon \cong 1 - \exp(-k^c W/\overline{\mu}) \qquad \text{(G5-2-4)}$$

where k^c is the wave-number-averaged mass absorption coefficient, and W denotes either LWP or IWP. $1/\overline{\mu}$ is referred to as the diffusivity factor, and a value of 1.66 is used.

In this model, k^c values of 0.158 for the downward emittance of water clouds and 0.130 for the upward one, computed by Stephens (1978), are used. For ice clouds, a k^c value of 0.06 (Liou, 1992) is adopted.